Nickel catalysts supported on carbon nanofibers: structure and activity in methane decomposition

Sh.K. Shaikhutdinov *, L.B. Avdeeva, B.N. Novgorodov, V.I. Zaikovskii and D.I. Kochubey

Boreskov Institute of Catalysis, Ak. Lavrentieva 5, Novosibirsk 630090, Russia
E-mail: shamil@catalysis.nsk.su

Received 21 March 1997; accepted 20 May 1997

Structures of Ni catalysts supported on filamentous carbon (CFC) produced by methane decomposition over coprecipitated Ni and Ni–Cu/alumina catalysts were studied by EXAFS and TEM. Thermal pre-treatment in N_2 at 350°C of samples impregnated by nickel nitrate precursor was found to produce either NiO or nickel carbide, Ni_3C, phase. This was explained by different reducing properties of the carbon nanofibers which depend on the surface structure. High stability of the Ni/C catalysts in methane decomposition reaction at 550°C was found with those prepared from only nickel chloride precursor, due to the formation of large (30–70 nm) Ni particles further leading to new carbon filaments growth. Data implies a common mechanism of the filamentous carbon deposition in all Ni-based catalysts, independent of the support (silica, alumina, carbon) being used. However, accumulation of filamentous carbon is strongly influenced by morphology and texture of the support.

Keywords: carbon, EXAFS, methane, nickel catalyst, nickel carbide

1. Introduction

Various carbon materials, e.g., charcoal, carbon blacks etc., are currently used for the preparation of metal catalysts (for a review, see ref. [1]). Recently, Baker et al. [2] and Geus et al. [3] have suggested carbon nanofibers as a novel support for catalyst preparation. Carbon nanofibers (or, more accepted term, ''carbon filaments'') are usually deposited on 3d-metal catalysts in reactions including decomposition or conversion of carbon-containing gases, e.g., methane, ethylene, CO, etc. [2–4,6].

Recently, we have studied the genesis and evolution of coprecipitated Ni and Ni–Cu catalysts with high metal loadings (up to 90 wt% Ni/alumina), which were developed in order to produce a huge amount of carbon (ca. 300 g_c/g_{cat}) by decomposition of methane as a main component of natural gas [5,6]. Transmission electron microscopy (TEM) studies of these and analogous catalytic systems showed a variety of carbon morphologies and stacking arrangements of graphitic platelets in carbon filaments depending on the catalyst and reaction conditions [2–4,6,7]. Graphene layers are oriented at some angle to the fiber axis in carbon produced by Ni catalysts, while the layers are perpendicular to the axis in those prepared by Ni–Cu catalysts of methane decomposition or steam reforming [6,7]. Recently, a high-resolution TEM study revealed that graphite edges were generally bent on the filament surface so that the basal planes are almost parallel to the filament axis in Ni catalysts. In Ni–Cu catalysts, the neighbour or next-neighbour layers were linked and formed ''closed-layers'' structures [7]. This surface reconstruction seems to be energetically favourable due to a lowering of the surface energy. Therefore, we expect some different behaviour in the interaction of the metal with the support in the preparation of carbon-supported Ni catalysts and, hence, of their activity.

In continuation of our long-term investigations, we have studied in this paper filamentous carbon as a support for Ni catalysts, in turn, aimed to further use in the methane decomposition reaction. The Ni/C catalysts, prepared from nickel nitrate and chloride, were characterized by TEM and extended X-ray absorption fine-structure spectroscopy (EXAFS).

2. Experimental

Carbon nanofibers were produced by coprecipitated 90 wt% Ni–alumina and Ni–Cu–alumina catalysts as described elsewhere [3]. The parameters of the carbon supports and their abbreviations are listed in table 1. (Note, that ''CFC'' means ''catalytic filamentous carbon''.) The Ni/C catalysts were prepared by wet impregnation of carbon granules (~ 0.2 mm mesh) using aqueous solutions of $Ni(NO_3)_2 \cdot 6H_2O$ and $NiCl_2 \cdot 6H_2O$ (reagent grade). Wet samples were kept in ambient conditions for 12 h and were subsequently dried at ~ 100°C for 2 h, followed by thermal treatment (calcination) in nitrogen at 350°C for 2 h. For catalytic tests, the samples were reduced in situ in H_2 flow (~ 1.2 ℓ/h) at 350–400°C for 3 h. Then, the temperature was increased up to 550°C with a rate of ~ 10°C/min prior to methane admission

* To whom correspondence should be addressed.

Table 1
The texture properties of the carbon supports and of carbon produced by Ni(c)/C catalysts in methane decomposition reaction at 550°C

Carbon abbrev. [a]	Catalyst	Surface area S_{BET} (m^2/g)	Pore volume (cm^3/g)
CFC-I [a]	90 wt% Ni/alumina	105	0.25
CFC-II	88 wt% Ni–8 wt% Cu/alumina	210	0.55
CFC-III	57 wt% Ni–23 wt% Cu/alumina	330	0.75
	15 wt% Ni(c)/CFC-I [b]	97	0.27
	15 wt% Ni(c)/CFC-II	115	0.29

[a] CFC means "catalytic filamentous carbon".
[b] Ni(c) means that the catalyst was prepared using nickel chloride precursor.

into the reactor. Methane of 99.99%, H_2 of 99.9% and N_2 of 99.9% purity grade were used. The activity measurements were carried out in a vibrating flow-reactor at atmospheric pressure of methane and at space velocity 70 $\ell/(g_{cat}h)$. Methane conversion was determined by gas chromatography. The reaction was followed until the complete deactivation of the catalysts in order to calculate the carbon capacity, G, i.e., grams of carbon deposited per gram of nickel.

TEM images were obtained with a JEM-2010 microscope operated at 200 keV. EXAFS spectra of Ni K-edge absorption were recorded at the Siberian Center of Synchrotron Radiation (Novosibirsk). Spectra were subjected to a common procedure to extract the oscillation part, $\chi(k)$. Fourier transform of $k\chi(k)$ data in the wave number range, $k = 2$–11 Å^{-1} was used to obtain a radial distribution of atoms (RDA). Computer simulations were done with EXCURV-92 software to calculate interatomic distances, R, coordination numbers, N, and Debye–Waller factors.

3. Results and discussion

For preparation of the Ni catalysts, we followed a usual way using nickel nitrate and chloride as precursors, abbreviated through the text as Ni(n) and Ni(c), respectively. In each step, we monitored the Ni state by EXAFS (figure 1, table 2). For reference, we also recorded a spectrum of the precursor powders used for the impregnating solution. The distance assignment was one using crystallographic data [8], i.e., $R_{Ni-Cl} = 2.40$ Å, $R_{Ni-O} = 2.09$ Å in nickel chloride, and $R_{Ni-O} = 2.06$ Å in nickel nitrate.

RDA curves of the samples, prepared from nickel chloride and supported on both CFCs and subjected to thermal treatment in N_2 at 350°C, show a main peak at ~ 2.4 Å (figure 1a) assigned to the Ni–Cl distance. We found that reliability factor $\mathcal{R}$ (the lower the $\mathcal{R}$-factor the better the fitting) was decreased if we assumed two Ni–Cl distances which were attributed to the two distinct sites for the Cl atoms in bridge and in "octa"-positions. This implies that the nickel phase is represented by a chain composed of $NiCl_4$–Cl_2 octahedra similar to that found in $NiCl_2 \cdot 2H_2O$ crystal [8]. However, a lower N value for the Ni–Ni distance (~ 3.5 Å) obtained with the CFC-II support means that in the calcined Ni(c)/CFC-II sample a $NiCl_2$ species is likely smaller than that supported on CFC-I.

As far as the nickel precursor was concerned, we expected the formation of the NiO phase after calcina-

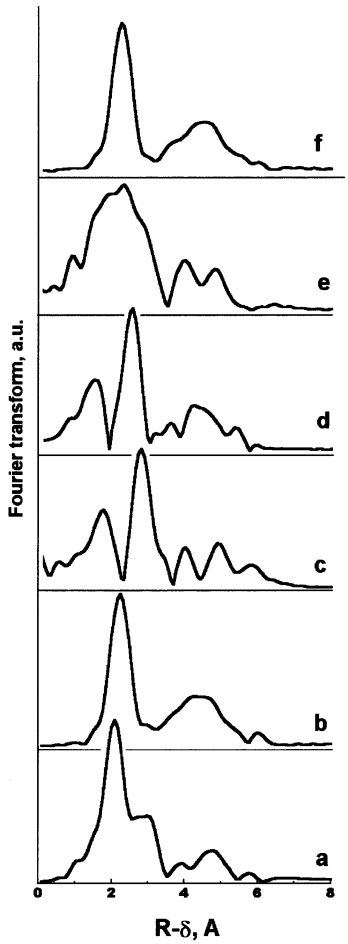

Figure 1. RDA curves of the Ni surrounding in: calcined and reduced Ni(c)/CFC-I,-II samples (a and b, respectively); calcined Ni(n)/CFC-I and Ni(n)/CFC-II samples (c and d, respectively); reduced Ni(n)/CFC-I,-II samples (e); Ni(n)/CFC-II sample exposed to methane decomposition reaction at 550°C for 40 min and subsequently cooled to room temperature (f).

Table 2
Parameters of RDA curves of the carbon-supported Ni catalysts

Sample	Atom pair	Distance (Å)	Coordination number, N	Debye–Waller factor $(Å^{-1})^2$	Nickel phase ($\mathcal{R}$-factor)
Ni(c)/CFC-I	Ni–Cl	2.32	3.0	0.010	Ni_2Cl_4
calcined	Ni–Cl	2.44	3.1	0.012	(22.0)
	Ni–Ni	3.43	4.2	0.019	
Ni(c)/CFC-II	Ni–Cl	2.31	3.8	0.021	Ni_2Cl_4
calcined	Ni–Cl	2.44	2.3	0.015	(17.0)
	Ni–Ni	3.46	2.3	0.025	
Ni(c)/CFC-I,-II	Ni–Ni	2.47	10.8	0.017	Ni
reduced	Ni–Ni	3.46	4.9	0.018	(21.5)
	Ni–Ni	4.27	10.2	0.015	
	Ni–Ni	4.72	16.0	0.017	
Ni(n)/CFC-I	Ni–O	2.07	4.2	0.008	NiO
calcined	Ni–Ni	2.95	8.6	0.013	(24.9)
	Ni–Ni	3.51	2.3	0.014	
	Ni–Ni	4.27	4.1	0.009	
	Ni–Ni	5.10	10.2	0.011	
	Ni–Ni	6.06	8.1	0.009	
Ni(n)/CFC-II	Ni–C	1.73	3.9	0.011	Ni_3C
calcined	Ni–Ni	2.68	9.2	0.019	(37.8)
	Ni–Ni	3.72	6.4	0.024	
	Ni–Ni	4.43	7.7	0.008	
	Ni–Ni	4.62	10.5	0.019	
	Ni–Ni	4.93	18.0	0.019	
Ni(n)/CFC-I,-II	Ni–O	2.08	5.6	0.020	Ni + NiO
reduced	Ni–Ni	2.47	5.9	0.018	(27.6)
	Ni–Ni	2.63	2.3	0.012	
	Ni–Ni	4.34	7.1	0.018	
	Ni–Ni	4.58	4.4	0.011	
Ni(n)/CFC-II	Ni–Ni	2.48	11.0	0.016	Ni
after 40 min in	Ni–Ni	3.44	4.5	0.022	(22.5)
reaction	Ni–Ni	4.28	7.4	0.009	
	Ni–Ni	4.74	12.4	0.012	

tion at 350°C, in accordance with general chemistry of nickel nitrate which decomposes at ca. 280°C. Indeed, the EXAFS spectrum was well fitted by the NiO phase supported on CFC-I (figure 1c). However, in the case of the CFC-II support, the RDA curve showed the absence of the Ni–O bond; instead we found a short distance ~ 1.7 Å (figure 1d). The best curve fitting was done assuming the nickel carbide phase, Ni_3C, with parameters presented in table 2. Therefore, data shows that at ~ 350°C in inert atmosphere, the C atoms of the support can interact with nickel nitrate during its decomposition.

Recently, Gandia and Montes [9] have found that the structure of the nickel phase supported on charcoal using nitrate precursor was strongly influenced by thermal pretreatment in nitrogen. They have detected a highly dispersed NiO phase in samples treated at 300°C but metallic Ni phase at 450°C. The latter fact was explained by reducing properties of activated charcoal towards NiO which, in turn, was produced by decomposition of nickel nitrate. In our experiments at 350°C, we likely "froze" the structure formed within C–NiO interaction. Therefore, the different nickel phases obtained on the two carbon supports, subjected to identical treatments, can be explained by a higher reducing activity of carbon in the CFC-II sample. It was found that the reduction of nickel by activated charcoal proceeds at much lower temperature than by graphite crystallites with inert basal planes [9]. Since the surface structure of CFC-I is likely represented by highly stepped basal planes, while on CFC-II the "closed-layer" structures seem to be predominant [7], we conclude that in the latter case the carbon atoms are more reactive towards nickel and this interaction occurs via dissolution of the C atoms into the NiO phase, thereby producing the intermediate nickel carbide-like phases.

It should be mentioned that diffusion of C atoms through a metal particle is one of the steps in the generally accepted scheme of carbon filament deposition on 3d-metals [2,3,6,10]. Although the existence of the surface nickel carbide on the Ni particles under reaction is assumed [11], however, to our knowledge, one did not observe a *bulk* Ni carbide phase in *post*-reacted samples at room temperature. The reason is that the Ni particles, super-saturated with carbon under the reaction conditions, decompose on the metal and carbon phases upon either cooling to room temperature or replacing the methane flow by helium [6]. In our case, thermal treatment was done at 350°C, i.e., at temperature lower than that of decomposition of bulk nickel carbide ($T_d \approx 400$°C). TEM inspection of these samples showed non-identified particles, with average size smaller than 5 nm in diameter. Therefore, we conclude that in addition to the relatively mild conditions, the stability of the nickel carbide particles produced this way is also attributable to their small size.

EXAFS spectra of the Ni(n)/CFC samples, reduced at 400°C and passivated, showed complex RDA curves which, however, could be deconvoluted on metal and oxide phases (figure 1e). Therefore, this indicates either an incomplete reduction of the Ni_3C and NiO phases formed by pre-treatment or a small size of the reduced Ni particles, where the passivated (oxidic) film gives a contribution comparable with that of the metal core phase. Meanwhile, for ''chloride'' samples reduced at 350°C, RDA curves clearly point out the metallic phase (figure 1b), with relatively large metal particle size as revealed by their coordination number values close to those found in metal foil (table 2). Indeed, TEM photographs of the reduced Ni(c)/CFC catalysts showed large metal particles (30–70 nm) and well-shaped Ni crystallites deposited on the carbon nanofibers as well as large agglomerates which are rather mixed with carbon filaments than being supported, because their sizes are larger than a fiber cross diameter (figure 2a). The latter species appear to be formed in the large pores of the carbon support. In contrast, we found only the small particles ($\sim$ 5 nm) randomly distributed over nanofibers in Ni(n)/CFC samples. Moreover, high-resolution TEM images of the ''nitrate'' samples showed that Ni particles were mainly deepened into the carbon bulk (figure 2b), which further indicates a strong nickel–carbon interaction during the above treatments likely because of the high affinity of Ni and C. However, the interaction of the NO_3^- and Cl^- ions with carbon support during preparation of the catalysts seems also to account for an explanation of the influence of the precursor on the resulting Ni particle size. It should be mentioned that a similar effect was found with oxide [12] and active carbon [13] supports, where the Ni particle size was higher for catalysts prepared from chloride precursor, although the precursors were reduced in hydrogen without precalcination step.

Catalytic properties of the Ni/C samples tested in methane decomposition are summarized in table 3. We used the life-time of the catalyst and the carbon capacity, G, as criteria of the catalyst's stability. Since G values were found not to be strongly affected by Ni loading in the 10–20 wt% range, we have presented data for $\sim$ 15 wt% Ni/C samples in order to reveal the influence of both support and precursor. One can see that, first, a higher carbon deposition was found with catalysts prepared from nickel chloride precursor. Second, G values are significantly higher for samples prepared with CFC-II and CFC-III supports produced by Ni–Cu catalysts (see table 1) when compared with CFC-I produced by Ni ones, i.e., the influence of the carbon surface structure is clearly seen.

Taking into account the EXAFS data, we can explain the high stability of the Ni(c)/CFC catalysts by the facts that, first, the reduction temperature can be lowered enough to completely reduce $NiCl_2$ species and, second, the large Ni particles are finally produced, up to 200 nm. The latter seems to be also crucial since there is likely an optimum Ni size (ca. 50 nm) for filament growth [6]. It is interesting to compare the TEM photographs of the ''chloride'' and ''nitrate'' Ni/CFC catalysts both after 40 min of reaction (figures 2c and 2d, respectively). One can see the new carbon filaments to be already well developed in figure 2c while some short carbon ''branches'' covering the parent carbon are only observed in figure 2d. In the latter case, one could attribute this behaviour to the incomplete reduction of the nickel phase in Ni(n)/CFC samples, however, an EXAFS inspection of the post-reacted sample reveals only a metal Ni phase of small size (figure 1f, table 2). In addition, the HREM image shown in figure 2e illustrates that this kind of carbonaceous deposits is represented rather by a carbon encapsulating the small Ni particles and which hardly can be described as filaments. Therefore, the Ni(n)/CFC catalysts are rapidly deactivated in the reaction studied and, as a result, carbon accumulation is small (table 3).

Surface area and pore volume of secondary carbon, accumulated until deactivation of the Ni(c)/CFC catalysts, were close to the values of CFC-I carbon, produced by Ni/alumina catalysts under identical conditions (table 1). Moreover, a global kinetics of the methane conversion over Ni(c)/CFC catalysts, shown in figure 3, is also very similar to that obtained on Ni/alumina catalysts [6]. Therefore, we conclude that the accumulation of carbon in the Ni(c)/CFC catalysts likely proceeds via the same way as in the Ni/alumina catalysts studied previously [5,6]. If so, following our general concept of the deactivation of Ni-based catalysts in methane decomposition [6], the texture properties of the growing carbon filaments should not be ignored in the total carbon accumulation process occurring over the Ni/C catalysts. Indeed, it seems that highly porous carbon supports (CFC-II, CFC-III) are more suitable for subse-

a

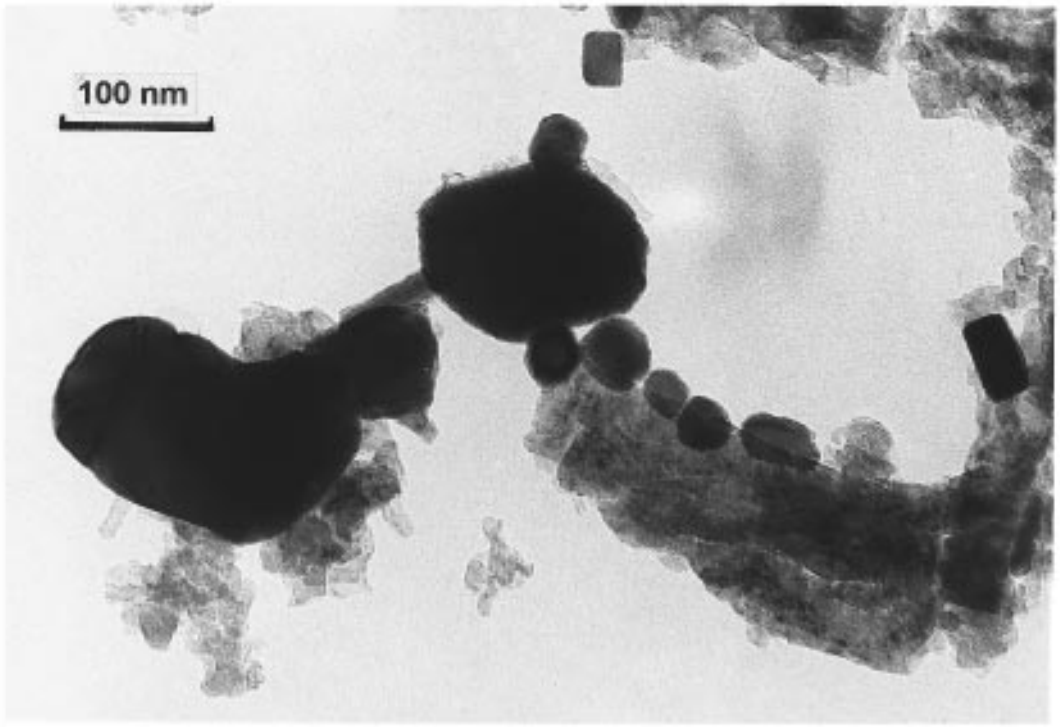

b

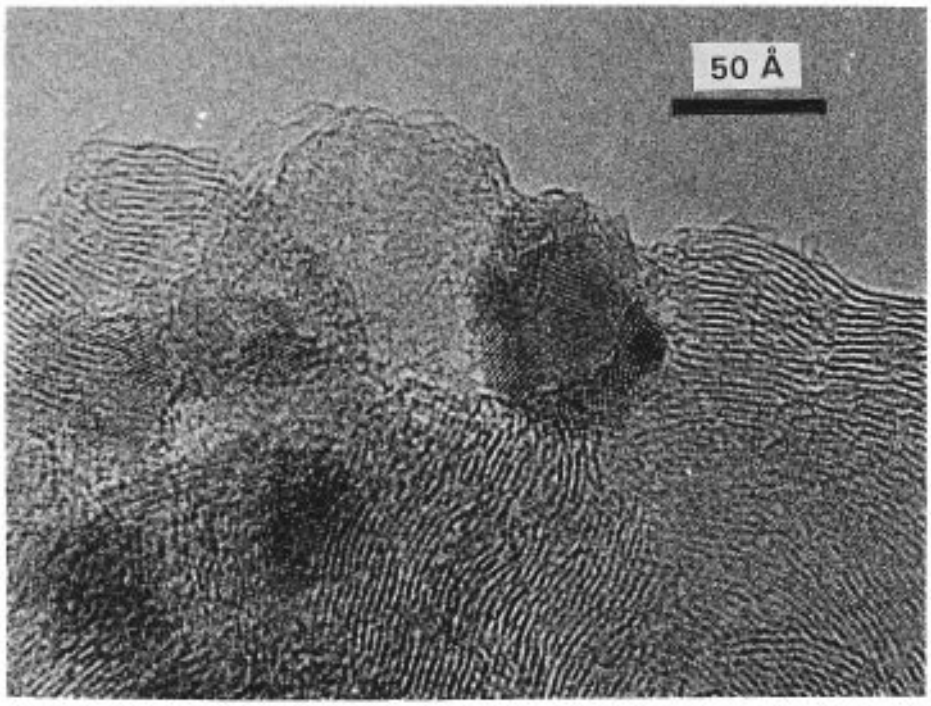

Figure 2. TEM photographs of the reduced Ni(c)/CFC-II (a) and Ni(n)/CFC-II (b) samples; (c) and (d) TEM photographs of (a) and (b) after 40 min in methane decomposition reaction at 550°C, respectively; (e) high-resolution image of post-reacted Ni(n)/CFC-II sample shown on (d).
(Continued on next page.)

c

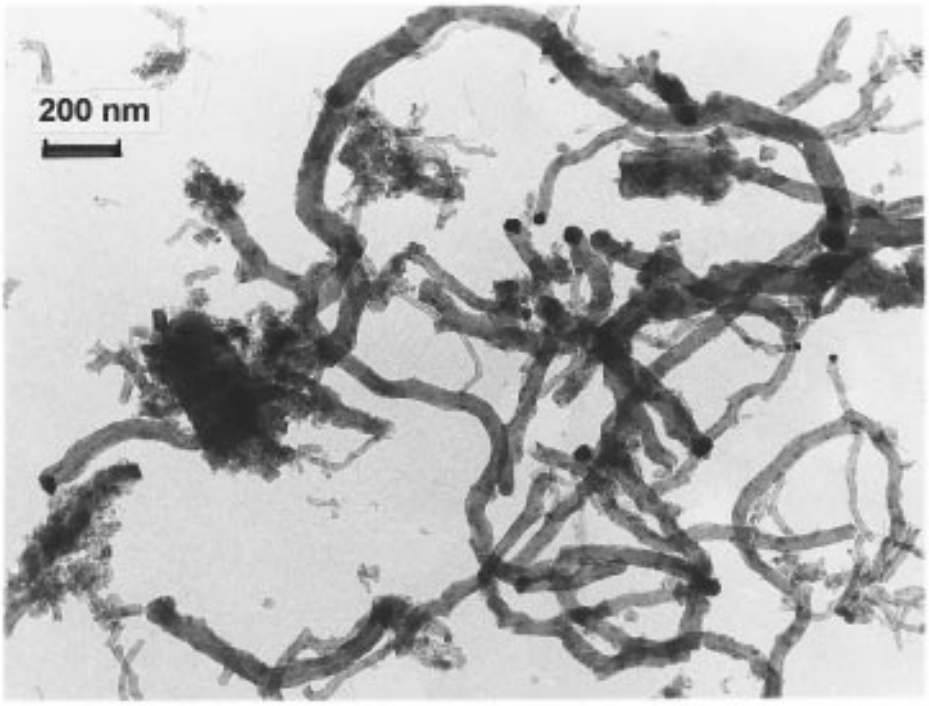

d

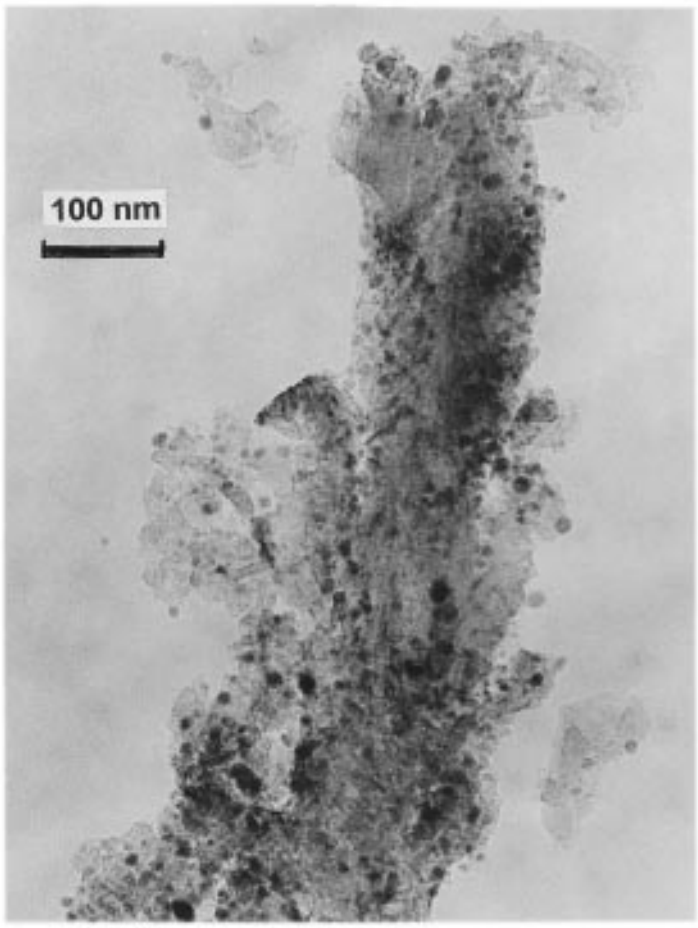

Figure 2. (Continued.)

e

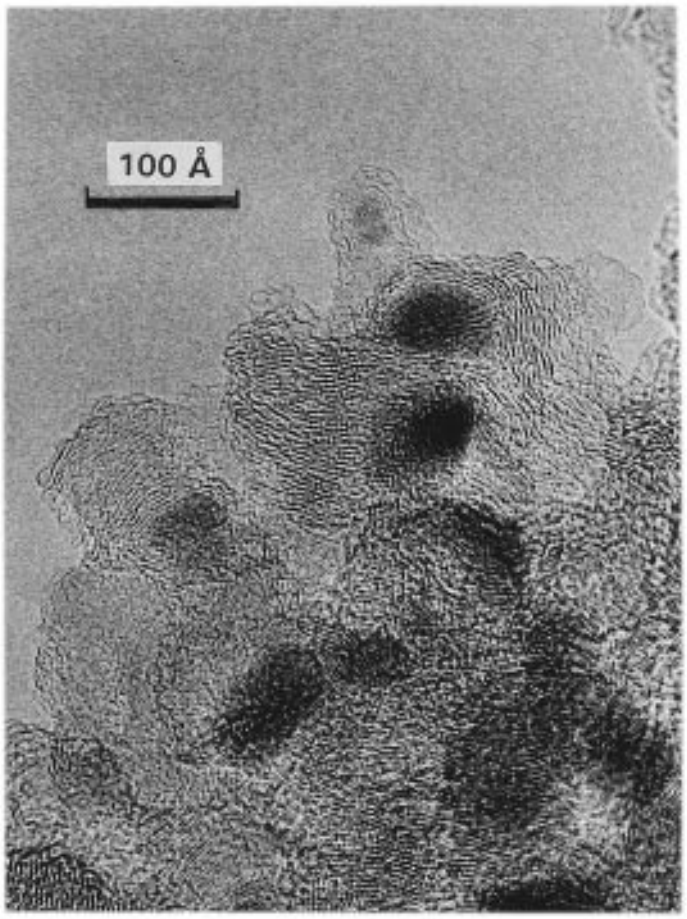

Figure 2. (Continued.)

quent new filament growth that, in turn, results in a higher carbon capacity value in comparison with a dense CFC-I one (table 3). However, surface area and pore volume are not the only parameters which determine the morphology of the carbon support. For instance, we have not found any activity in Ni catalysts supported on graphitic carbon "Sibunit", despite the high surface area (~ 300 m^2/g) and a relatively large metal particle size (~ 28 nm) produced using chloride precursor. The reason is that this support is known to be represented rather by holey egg shells [14]. In the latter samples, TEM examination showed that Ni particles were mostly located inside the shells and, hence, there was no free space for filament growth. Moreover, due to this structure, there are likely also some diffusion limitations for a gas flow. Therefore, we feel that for the reaction studied, this support is hardly acceptable.

Baker et al. [15] and Wolf et al. [16] have also observed Ni-catalysed carbon filaments in a hydrocarbon + H_2 flow at ~ 600°C when supported on PAN-based fibers. Therefore, on the basis of those and our evidences, we believe that the shape of the metal particle and graphite stacking in carbon filaments are inherent to hydrocarbon/Ni interaction solely and likely not affected by the

Table 3
Catalytic properties of the 15 wt% Ni/C catalysts in methane decomposition ($T = 550$°C, sample weight = 0.1 g, methane pressure = 1 atm, methane flow = 7 ℓ/h)

Carbon support	Nickel precursor	Catalyst "life-time" (h)	Methane conversion (%)	Carbon capacity, G (g_C/g_{Ni})
CFC-I	chloride	2	8	33
	nitrate	~ 2	6	22
CFC-II	chloride	17	8.5	245
	nitrate	5	7.5	40
CFC-III	chloride	13.5	4.5	210
Sibunit (~ 300 m^2/g)	chloride	–	~ 1	28

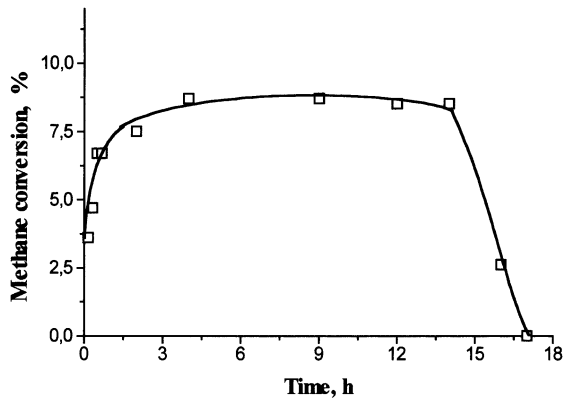

Figure 3. Global kinetics of methane conversion over 15 wt% Ni(c)/CFC-II catalysts (550°C, methane pressure = 1 atm, space velocity 70 ℓ/(g h)).

nature of the support. This implies a common mechanism of the initial growth of carbon filaments on all the Ni catalysts, independent of the support used. However, its accumulation is strongly influenced by morphology and texture of the support.

4. Conclusion

Nickel catalysts, supported on filamentous carbon (nanofibers), were prepared using nickel chloride and nitrate precursors and studied by EXAFS and TEM. Thermal pretreatment in N_2 at 350°C of samples, impregnated by nickel nitrate, caused the formation of either the NiO or nickel carbide, Ni_3C, phases. This was explained by different reducing properties of carbon which, in turn, depends on the structure of the filament surface.

The Ni/CFC catalysts were tested in methane decomposition reaction at 550°C. A high stability of the Ni/CFC catalysts was found with those prepared only from nickel chloride precursor. The global catalytic performances of the Ni(c)/CFC catalysts was similar to the Ni/alumina ones. This implies a common mechanism of the carbon filament growth on all the Ni catalysts, independent of the support (alumina, silica, carbon) being used. However, its stability towards carbon accumulation seems to be strongly influenced by morphology and texture of the support.

We believe, that carbon nanofibers could be used as a promising support for preparation of carbon-supported metal catalyst. It seem reasonable that noble metals, where metal–carbon affinity is not so pronounced as in 3d-metals, will be more suitable for these purposes. This work is now in progress.

Acknowledgement

The authors gratefully thank Professor V. Fenelonov for texture data of the carbons studied.

References

[1] R. Burch, ed., *Proc. 1989 Meeting on Carbon and Catalysis*, Loughborough 1989, Catal. Today 7 (1990).
[2] M.-S. Kim, N.M. Rodriguez and R.T.K. Baker, in: *Synthesis and Properties of Advanced Catalytic Materials*, MRS Symp. Proceeding, Vol. 368, eds. E.I. Iglesia, P.W. Lednor, D.A. Nagaki and L.T. Thompson (1995) p. 99.
[3] J.W. Geus, A.J. van Dillen and M.S. Hoogenraad, in: *Synthesis and Properties of Advanced Catalytic Materials*, MRS Symp. Proceeding, Vol. 368, eds. E.I. Iglesia, P.W. Lednor, D.A. Nagaki and L.T. Thompson (1995) p. 87.
[4] C.A. Bernardo, I. Alstrup and J.R. Rostrup-Nielsen, J. Catal. 96 (1985) 517.
[5] Sh.K. Shaikhutdinov, L.B. Avdeeva, O.V. Goncharova, D.I. Kochubey, B.N. Novgorodov and L.M. Plyasova, Appl. Catal. A 126 (1995) 125.
[6] L.B. Avdeeva, O.V. Goncharova, D.I. Kochubey, V.I. Zaikovskii, L.M. Plyasova, B.N. Novgorodov and Sh.K. Shaikhutdinov, Appl. Catal. A 141 (1996) 117.
[7] Sh.K. Shaikhutdinov, V.I. Zaikovskii and L.B. Avdeeva, Appl. Catal. A 148 (1996) 123.
[8] B. Morosin, Acta Cryst. 23 (1967) 630.
[9] L.M. Gandia and M. Montes, J. Catal. 145 (1994) 276.
[10] I. Alstrup, J. Catal. 109 (1988) 241.
[11] A.J.H.N. Kock, P.K. de Bokx, E. Boellard, W. Klop and J.W. Geus, J. Catal. 96 (1985) 468.
[12] C. Hoang-Van, Y. Kachaya, S.J. Teichner, Y. Arnaud and J.A. Dalmon, Appl. Catal. A 46 (1989) 281.
[13] M. Domingo-Garsia, L. Vicente-Gutierrez and C. Moreno-Castilla, React. Kinet. Catal. Lett. 43 (1991) 93.
[14] Y.I. Yermakov, V.F. Surovkin, G.V. Plaksin, V.A. Semikolenov, V.A. Likholobov, A.V. Chuvilin and S.V. Bogdanov, React. Kinet. Catal. Lett. 33 (1987) 435.
[15] P. McAlister and E.E. Wolf, Carbon 30 (1992) 189.
[16] W.B. Downs and R.T.K. Baker, Carbon 29 (1991) 1173.